The 6th International Supercritical CO_2 Power Cycles Symposium
March 27 - 29, 2018, Pittsburgh, Pennsylvania

Advanced Regulatory Control of a 10 MWe Supercritical CO_2 Recompression Brayton Cycle towards Improving Power Ramp Rates

Priyadarshi Mahapatra
National Energy Technology Laboratory
Pittsburgh, PA 15236
Priyadarshi.Mahapatra@netl.doe.gov

Jacob Albright
National Energy Technology Laboratory
Morgantown, WV 26507
Jacob.Albright@netl.doe.gov

Stephen E. Zitney
National Energy Technology Laboratory
Morgantown, WV 26507
Steve.Zitney@netl.doe.gov

Eric A. Liese
National Energy Technology Laboratory
Morgantown, WV 26507
Eric.Liese@netl.doe.gov

ABSTRACT

As an attractive alternative to conventional Rankine cycles utilizing sub/supercritical steam, Brayton power cycles utilizing supercritical carbon dioxide (sCO_2) offer the potential for significant operational and capital cost benefits. The high density of the sCO_2 working fluid allows for highly compact turbomachinery and a power cycle with potentially higher thermal efficiencies and lower overall cost of electricity. Due to these advantages over traditional systems, the U.S. Department of Energy, under its Supercritical Transformational Electric Power Program, has awarded a project to design, build and operate a nominal 10 MWe (net) recuperated sCO_2 Brayton recompression cycle test facility to accelerate scale-up, development, and commercial deployment. In this paper, a previously designed commercial simulation software-based dynamic process model of a 10MWe indirect recuperated sCO_2 recompression Brayton cycle is used to develop advanced regulatory controllers for efficient performance in the face of fast load-demand and natural gas fuel-availability ramp-rates.

sCO_2 cycle efficiency is strongly dependent on maintaining a high turbine-inlet-temperature (TIT) based on material constraints and a low main compressor inlet temperature (MCIT) near the critical point of CO_2. This study, which assumes grid-connected coupled turbomachinery, uses inventory control wherein sCO_2 is removed from the closed cycle and stored in an inventory-tank to maintain the TIT during power turndown (part-load operation). During a subsequent fast power turn-up when sCO_2 in the tank is put back into the cycle, the TIT tends to overshoot the maximum allowable temperature constraint due to inherent delays in TIT response to load changes. Motivated by this, an advanced controller logic is developed that regulates the inventory inlet and outlet valves in a fast and effective manner to achieve the TIT control objective while satisfying process constraints. Similarly, the MCIT is tightly regulated to operate at its design point slightly above the critical CO_2 temperature, thereby avoiding transition to the two-phase region at the compressor entry point. In addition, the sCO_2 cooling water outlet temperature is actively controlled with an upper constraint, to prevent scaling issues. Moreover, based on previous open-loop investigations for determining flow-split criteria of the main compressor and bypass compressor streams, a controller is designed that aims at maximizing cycle efficiency based-on such criteria during transient operations. This paper presents various load and natural gas fuel turn-down results and critical analysis of trade-offs between cycle efficiency and control system performance. Finally, the paper will conclude with brief discussion on control configuration changes for a grid-independent “island” operation, which utilizes a turbine inlet throttle-valve for turbine-speed control as an indirect augmentation to TIT control using sCO_2 inventory.

KEYWORDS: Supercritical CO_2, Dynamic Simulation, Regulatory Control, Cycle Efficiency, Load Following, Part-Load Operation, CO_2 Inventory, Fast Ramp-Rates

INTRODUCTION

Closed-loop Brayton cycles with supercritical carbon dioxide (sCO_2) as the working fluid are gaining increased visibility as an attractive alternative to conventional steam-based Rankine cycles (Ahn et al., 2015; Dostal et al., 2006). As an exploratory test and research platform for demonstrating potential advantages of this technology (Pasch et al., 2012; Conboy et al., 2013), the U.S. Department of Energy (DOE), under the auspices of the Supercritical Transformational Electric Power (STEP) program, has awarded a project to design, build and operate a nominal 10 MWe pilot plant facility to accelerate the scale-up, development, and deployment of commercial sCO_2 Recompression Closed Brayton Cycle (RCBC) technologies (DOE, 2015). RCBCs present unique operational challenges due to the high degree of heat recuperation and pressure interactions between the low- and high-pressure sides of the power cycle. It is also necessary to control RCBC response to various anticipated disturbances, while maintaining operation with the CO_2 working fluid in the supercritical region, especially near highly nonlinear states at the cooler exit and main compressor inlet. Recent steady-state analysis and sensitivity studies at the National Energy Technology Laboratory (NETL) have examined sCO_2 RCBC performance with an emphasis on cycle efficiency (White, 2014; White et al., 2014).

There are limited studies in literature which emphasize how to address RCBC operational and control challenges. One of the key research efforts underway on the subject by Argonne National Lab (ANL) (Moisseytsev and Sienicki, 2006; Moisseytsev and Sienicki, 2008, Moisseytsev and Sienicki, 2009 and Moisseytsev and Sienicki, 2011), which is using the in-house ANL Plant Dynamics Code to investigate the control strategy effectiveness for a 96 MWe Lead-Cooled Fast Reactor-based sCO_2 Brayton cycle. The controllers were tested for 3%/min linear change in grid demand from full-power to any power level and found adequate in accommodating such changes. However, it was noted that the return to full power was studied at slower rates and were ramped up from 50% of full-power, instead of very low load conditions. In addition, the study also notes a small amount of non-steady behavior at the point of return to full power. Moisseytsev and Sienicki (2008) provide further analysis of the sCO_2 cycle for conditions not covered in the previous study, especially related to oscillating cycle behavior as calculated by the ANL plant model. The oscillations and unsteady behavior were attributed to the non-rigorousness of underlying compressor models. It also includes compressor surge control via a reliable surge prediction criterion. Moisseytsev and Sienicki (2009) report further improvement to the previous studies where an optimal control strategy based on steady-state, quasi-static, and dynamic calculations was developed which relies on a turbine bypass for generator output control, assisted by inventory control in the 30%-90% load range in order to operate at good efficiency at reduced loads. The study demonstrates that the developed control strategy is able to control the cycle over the entire range of generator load (0%-100%). In Moisseytsev and Sienicki (2011), the authors report that with turbine bypass, the cycle efficiency reduces almost linearly with the grid demand, while the inventory control provides the most efficient operation at reduced loads.

At MIT, Carstens (2004) developed a code called Gas Plant Analyzer and System Simulator/CO2 (GAS-PASS/CO2) that models the sCO_2 recompression cycle. For transient solutions, perfect mixing assumption and the quasi-static momentum equation were assumed. Utilizing this model, Carstens investigated part-load operation using combined inventory and low temperature control, low temperature control only, high temperature control, turbine throttling, turbine bypass, turbine and integrated heat-exchanger bypass and upper-cycle bypass. They concluded that the combined inventory and low temperature control is the most efficient operation method with better controllability over the full operational range of the cycle. However, the fully-implicit solution method used in GAS-PASS/CO2 code can be computationally expensive and increases simulation run-time. Moreover, their simplifying assumptions may cause non-physical solutions. Also from MIT, the SCPS code (Kao et al, 2009) makes less assumptions and models fluid properties more accurately within component control volumes. The momentum integral model, utilizing NIST REFPROP subroutines and tables, is used to solve the conservation equations for the integrated system. A semi-implicit scheme is implemented to determine system behavior. SCPS code models and assumptions make it more appealing for use in determining sCO_2 Brayton cycle dynamic behavior. The control architecture was developed to maintain compressor inlet conditions away from and above the pseudo-critical region. The study used turbine throttle and bypass control to achieve a controlled power output and claimed to successfully control the sCO_2 cycle for a wide range of operational transients. The primary limitation to this study is the over-simplistic non-pressure-driven equipment models. In addition, low variations to power demand cases were studied and wide operation ranges could not be ascertained. More importantly the SCPS code models a simple Brayton cycle layout versus the RCBC layout. Hence in another MIT study, Trinh (2009) extended Kao's SCPS code directly for an RCBC layout and named the code Transient Supercritical Cycle Code (TSCYCO). Trinh investigated a 600 MWth (254 MWe) RCBC model with a turbine inlet temperature of 650°C (923.2 K) and a compressor inlet temperature of 35.25°C (308.4 K) with various transient studies close to steady-state operation and 10% steps in loss of load (LOL) simulations. Various control models including flow-split valve control, bypass valve control, low-temperature control, and inventory control were utilized during the transients. The control models were reported to perform well, however TSCYCO was reported to experience instabilities when operated too close to the CO_2 critical point.

Other control studies for sCO_2 Brayton cycles have been reported with various heat sources. Singh et al. (2011) developed a control-oriented modular DYMOLA simulation-based dynamic model of the power-loop using zero- and one-dimensional thermal-hydraulic mathematical models of components. Proportional Integral (PI)-based controllers were implemented for compressor inlet pressure using a theoretical sCO_2 mass addition (as opposed to an inventory tank) and compressor inlet temperatures using cooling-medium mass flow regulation. Responses to step increases in heater power by ~20% changes were reported. Casella and Colonna (2011) developed a Modelica-based dynamic model of solar-powered sCO_2 Brayton cycle power plant for control studies, wherein preliminary simulations of open-loop transients corresponding to changes in cycle CO_2 holdup, cooling water flow, solar energy input and turbine bypass valve opening were conducted. No closed-loop control simulations were reported.

In the current study, a detailed regulatory-based control architecture has been implemented on a rigorous pressure-driven 10MWe RCBC dynamic process model previously developed at the National Energy Technology Laboratory (NETL) by Zitney and Liese (2018). The intent for this study is to provide rigorousness to the control design methodology and to aid the control community in better understanding the nuances involved in operating and controlling this next-generation power cycle technology. The key control responses are presented for large manipulations in typical MW demand and fuel flowrates. The following section presents the control methodology used in this study wherein the control objectives, proposed control architecture to meet these objectives and the simulation test bed have been described. The subsequent section gives the results and discussions based on the dynamic simulation responses for three relevant case studies. The paper concludes with a brief discussion on inventory tank pressure-pinch case and a brief highlight of future work.

CONTROL METHODOLOGY

From the underlying Carnot efficiency law, it can be deduced that keeping the turbine inlet temperature (TIT) as close as possible to its maximum design temperature (973.2 K) and the main compressor inlet temperature (MCIT) as close as possible to its minimum design temperature (306.6 K) is crucial to maximizing cycle efficiency. While this is true for steady-state operation at part-load and full-load conditions, satisfying similar criteria during dynamic operations, such as work-load / fuel ramps, ensures high cycle efficiency during these transients. In addition, certain process constraints such as compressor-surge avoidance, cooling water exit temperature not exceeding calcification temperature, and TIT not going above an upper limit based on material constraints must be strictly enforced throughout the transient operations. These criteria necessitate the design of controllers that can handle such constraints critical for safe operation and minimizing equipment damage, especially during rapid transitions. In addition, meeting the cycle MW demand, maintaining cycle efficiency and rejecting process disturbances such as fuel availability/heating value is crucial.

Control Objectives

In this sub-section, the regulatory-layer control objectives are described based on the above control problem statement(s). The term "regulatory-layer" is used in the context of maintaining a certain desirable condition without dynamically evaluating process variables to meet certain optimization criteria such as minimizing settling times, utility usage, etc. – the latter control philosophy lies within the purview of "supervisory-layer" control architecture and is beyond the scope of this work. Note that satisfying some of proposed regulatory objectives also ensure stable operation. The following list presents the primary control objectives used in this study, based on the above discussion:

- Given that the sCO_2 RCBC dynamic model is fully pressure-driven (similar to real plant processes), various feed-streams are flow-controlled to maintain a desired flowrate in the face of upstream/downstream pressure fluctuations.

- The natural gas (NG) combustion process takes place at a specific pressure and hence the combustion-reactor is pressure controlled. This ensures the mass balance around the reactor furnace.

- The NG combustion furnace is temperature controlled to ensure the desired reaction kinetics and to avoid equipment damage

- The TIT is maintained at 700°C (973.2 K) to ensure maximum cycle efficiency, as described earlier. However, the TIT should not exceed 715°C (988.2 K) to prevent material damage to turbine components.

- Prevent main and bypass compressor surge by enforcing surge-margin lower-constraint to 10% above surge limit.

- Maintain main and bypass compressor flowrate split-ratio to maximize cycle efficiency. This criterion is based on previous steady-state off-design studies (Zitney and Liese, 2018) and is also discussed later in the text.

- Meet net-work demand (for load-following scenarios, described later in the text).

- Maintain MCIT at 2.5 degrees above the subcritical limit, i.e., at 306.6 K. Based on previous steady-state analysis (Zitney and Liese, 2018) it was found that a slight increase in this temperature introduces significant penalty to the cycle efficiency. On the other hand, decrease in this temperature carries the risk of sCO_2 entering a subcritical 2-phase region which may be detrimental for compressor operation.

- Prevent cooling water exit temperature from exceeding calcification temperature of 50°C (323.6 K).

In many of the prior studies (Carstens, 2004; Trinh, 2009), a turbine throttle control has been used to control generator power which in turn matches the reactor power/heat source and the turbine MW demand. However, in this study no turbine throttle has been utilized and a direct conversion of heat-source enthalpy into turbine MWs based on a fixed turbomachinery “grid” speed is assumed.

Control Architecture

Figure 1 shows the process flow diagram (PFD) of the sCO_2 RCBC, along with the regulatory control implementation. The color-coded round blocks represent different PI-based controller types including flow control (green), temperature (red), pressure control (purple) and work control (yellow). The dotted lines represent control signals which are indicative of process variables (PVs), control output / manipulated variables (MVs) and setpoint (SP) signals. Whether a signal represents a PV/SP or an MV can be inferred from the direction/arrows on the lines. A PV/SP signal points towards a controller block whereas MV points away from the controller typically towards an actuation device such as valve or another cascaded controller block (SP for the cascaded block).

The following list provides more detail for the individual controllers. It must be noted that most of the controller blocks are PI-based unless mentioned otherwise.

1. Flow Controller (FC) to regulate air-flow measures mass flowrate of air entering the air-blower and manipulates the blower load. The SP to this controller is provided by a fuel/air ratio block described later.

2. FC to regulate NG-flow measures mass flowrate of NG and manipulates the valve position on the NG stream entering the combustion reactor. The SP is provided by work/fuel ratio block described later.

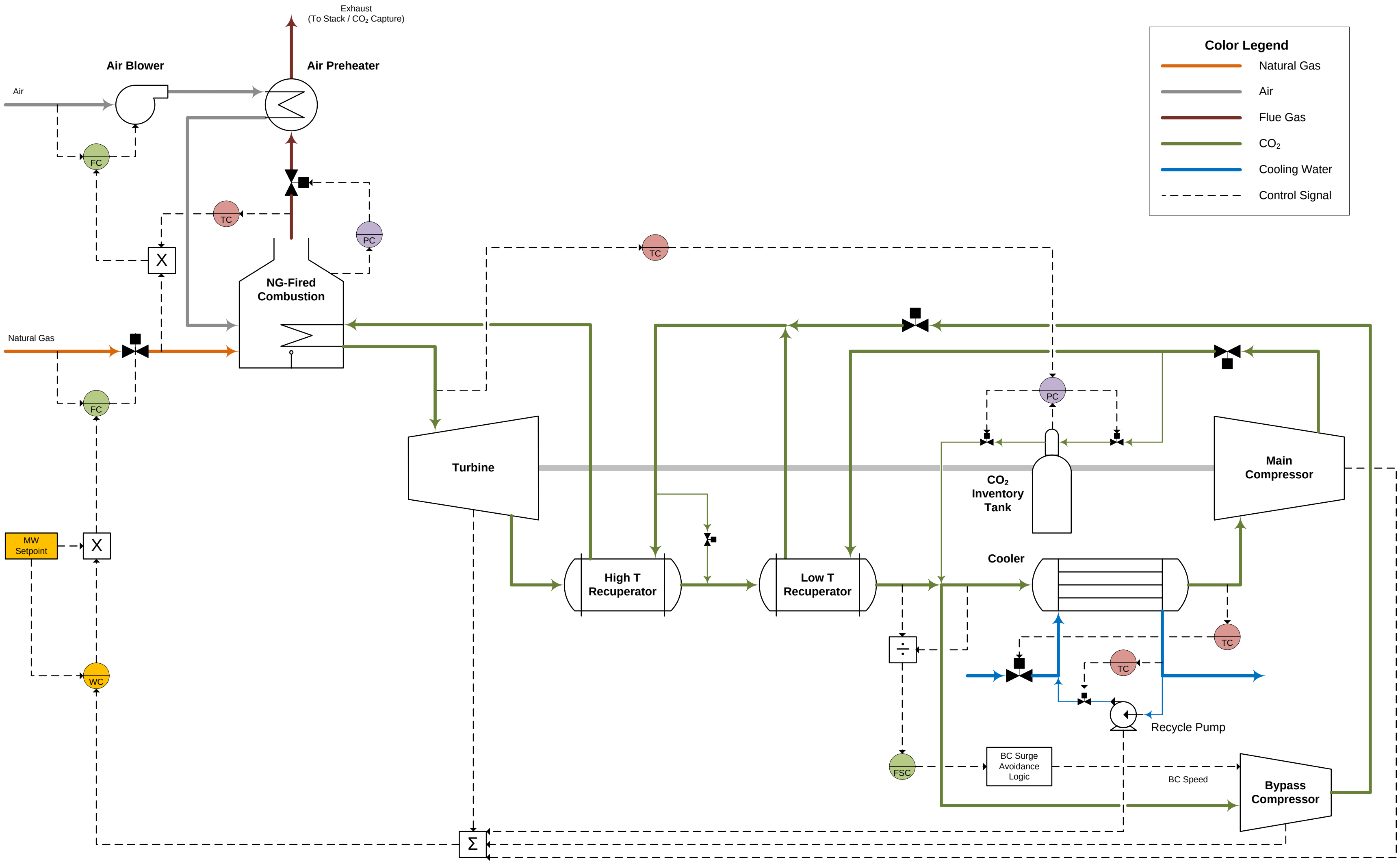

Figure 1. Process flow diagram (PFD) of the sCO_2 Brayton recompression cycle showing regulatory controllers

3. Pressure Controller (PC) to regulate combustion-reactor pressure measures reactor pressure and manipulates valve position on the reactor product line.

4. Ratio block to calculate air flow proportional to fuel flow. The output of this block is sent as SP to air FC.

5. Temperature Controller (TC) to maintain combustion-reactor temperature measures the temperature of reactor-product stream and manipulates/trims the air-to-fuel ratio.

6. PC to regulate sCO_2 inventory tank pressure uses a Split-Range control philosophy and sends control actuation signal to both inlet and outlet valves of the inventory tank (which are closed at initial conditions). It measures the difference of the pressure SP signal provided by the TIT controller (described later) and the actual tank pressure. If the difference is positive, only the inlet valve is opened proportional to the SP-PV difference, introducing sCO_2 into the tank (and therefore removing sCO_2 from the cycle) corresponding to a higher pressure SP. On the other hand, a negative SP-PV signal opens the outlet valve (with the inlet valve fully closed) removing sCO_2 from the tank back and putting it back into the cycle. A small pressure band is provided as a bias above/below which the valve actuation is initiated. This prevents jittering, i.e., frequent open-close operation, when SP-PV signal is close to zero.

7. TC to maintain the TIT at its design value of 700°C (973.2 K) measures temperature of the stream entering the turbine and manipulates the pressure SP provided to the inventory tank PC.

8. Flow-Split Controller (FSC) to maintain main-bypass flowrate split-ratios measures the flow-split fraction (MC-line flowrate / Total flowrate). The controller manipulates the flowrate through the bypass compressor line by actuating the BC-speed setpoint. This criterion is relaxed as the bypass compressor approaches surge margin using a surge-avoidance logic as shown in Figure 1. It must be noted that FSC being active/inactive forms the basis for comparative case studies described in the results and discussion section.

9. Ratio block to calculate NG flow proportional to net-work SP. The output of this is sent as SP to NG FC.

10. Work Controller (WC) to meet the net-work demand as provided in the MW-setpoint block measures the actual net-work, given by gross turbine power minus the power consumed by both compressors and cooling-water recycle pump, and manipulates/trims the fuel to work-demand ratio.

11. TC to regulate MCIT at 306.6 K measures the MCIT and manipulates the valve on the cooling water inlet line.

12. TC to regulate cooling water exit temperature below 50°C (323.6 K) measures the cooling water temperature exiting the cooler (cold-side) and manipulates the valve on the cooling water recycle line.

All the PI-controller tuning parameters have been calculated using both the Cohen-Coon method (open-loop test, conducted using +/- 10% step actuations in MV) and the Tyreus-Luyben method (closed-loop P-control test, using +/- 10% actuations in SP) and average heuristic values for controller-gain (Kc) and integral-time (τ_I) have been chosen. In addition, the TIT TC, the inventory-tank PC and WC, which involve relative slower responses (compared to regulatory FCs), are tuned with the "lower" regulatory FCs and cooler-related TCs in closed-loop.

Simulation Methodology

To study the controller performance, pressure-driven dynamic simulations of the 10MWe sCO_2

recompression Brayton Cycle were conducted using Aspen Plus Dynamics (Aspen Technology, 2017c). The regulatory control architecture was implemented within the Aspen Plus Dynamics (APD) graphical user interface. The controller logic used herein including PID-control blocks, control logic blocks involving ratio/multiplication calculations, evaluating hi/low among multiple signals, “delta” calculations, split-range control, etc., was incorporated directly within APD utilizing the in-built control-model(s) library.

The dynamic simulations were conducted on an Intel Core i7 (8-cores)-based Processor with a 64-bit Windows 7 workstation. APD V8.8 (Aspen Technology, 2017c) as part of the Aspen Technology V8.8 software suite was used as the dynamic simulation environment. Custom models for microchannel tube-based low-temperature recuperator (LTR) and high-temperature recuperator (HTR) were developed in Aspen Custom Modeler V8.8 (Aspen Technology, 2017a) and later imported within the APD model of the sCO_2 cycle. The dynamic integrator used a 5^{th} order variable-step Gear method (available in APD) with a relative convergence tolerance of 0.0005 and minimum step size of $1x10^{-5}$ hr. A mixed-Newton method available in APD was used to solve the nonlinear equations systems at each time step.

RESULTS AND DISCUSSION

This section presents sCO_2 RCBC dynamic simulation results for three case studies utilizing the above-described control-architecture. The first involves simulations with large ramp rates in MW-demand with active FSC. In the second case study, results for no flow-split control are compared to the previous case (with active FSC). The third case study presents cycle responses to large ramp rates in NG flowrates.

Control responses for large-ramps in MW demand

This section presents simulation results for 3%/min ramps in MW load demand in the presence of FSC. Figure 2 shows the MW-demand ramp-down, introduced at t = 1 hr, from 10 MW to 2.8 MW (72% turn-down) in a span of 0.4 hr. The cycle is held at this low-load condition until the process stabilizes. Thereafter, a ramp-up in MW demand is introduced at t = 7 hr with similar ramp-rate up to full-load condition. It can be seen that the actual net-work closely follows the MW demand, with the exception of the trailing end of the ramp up/down operation.

It can also be observed that during ramp-down, the efficiency briefly spikes to 48% (from around 46% at the design condition) due to the actual net-work generated decreasing at a lower rate compared to the fuel heat availability. However, as the TIT decreases (see Figure 3), the efficiency drops down to 31%. This later recovers and settles down at 40% as the TIT is restored by the TIT TC utilizing removal of sCO_2 from the cycle for storage in the inventory tank (Figure 5). During a ramp-up operation, the efficiency initially plummets to 35% within the first few minutes but rapidly ascends primarily due to increased TIT (Figure 3). This temperature is restored to design value by injecting sCO_2 from the inventory tank back into the cycle. It must be noted that the TIT peaks at 985K, which is below the upper constraint of 715°C (988.2 K), discussed earlier as a control objective. Figure 3 also shows that the combustion-reaction temperature serving as the heat-input for the entire cycle is well controlled.

Figure 4 shows the cooler temperature profiles corresponding to the ramp operations. As evident from the plots, the cooling water outlet temperature (green solid) rapidly rises during turn-down conditions. However, as this temperature reaches the upper constraint of 50°C, the cooling water recycle (pink solid) starts, successfully keeping the cooling water (CW)-outlet temperature below the constraint margin. At the same time, the overall CW flowrate which controls the sCO_2 MCIT (or the cooler hot-side exit temperature), decreases substantially keeping the net CW usage low. The MCIT can also be seen to be well controlled with a net variation of 1.5 K during the entire ramp operation.

Figure 5 results demonstrate how the sCO_2 gas is diverted into the inventory tank during ramp-down conditions by opening the inlet valve, thus increasing the inventory pressure. On the other hand, the sCO_2 cycle pressure (both the high and low-pressure sides) decreases owing to a decrease in holdup of the sCO_2 working fluid in the cycle. On the other hand, during ramp-up, the sCO_2 is put back into the cycle thereby reducing tank pressure (and restoring cycle pressures toward their design values). The split-range controller logic ensures that both valves are never open at any time, which may otherwise lead to continuous gas flow across the inventory tank.

Lastly, Figure 6 provides plots for surge and stonewall margins through the ramp operations. In the presence of FSC, the bypass-compressor shaft-speed is reduced during ramp-down operation to maintain the main-bypass flow-split ratio (see Figure 3). This leads to diverting some of the sCO_2 toward the main compressor (MC) and hence the bypass compressor (BC) moves towards surge (very close to surge-margin constraints of 10%), indicative of low flowrates corresponding to the operating pressure ratios. However, neither of the compressors violates the surge / stonewall margin during the ramp-operations. In the event BC surge-margin would have decreased below 10%, the BC surge-avoidance logic would have prevented further BC shaft-speed reduction by relaxing the FSC. However, in this study, such a constraint violation is not observed.

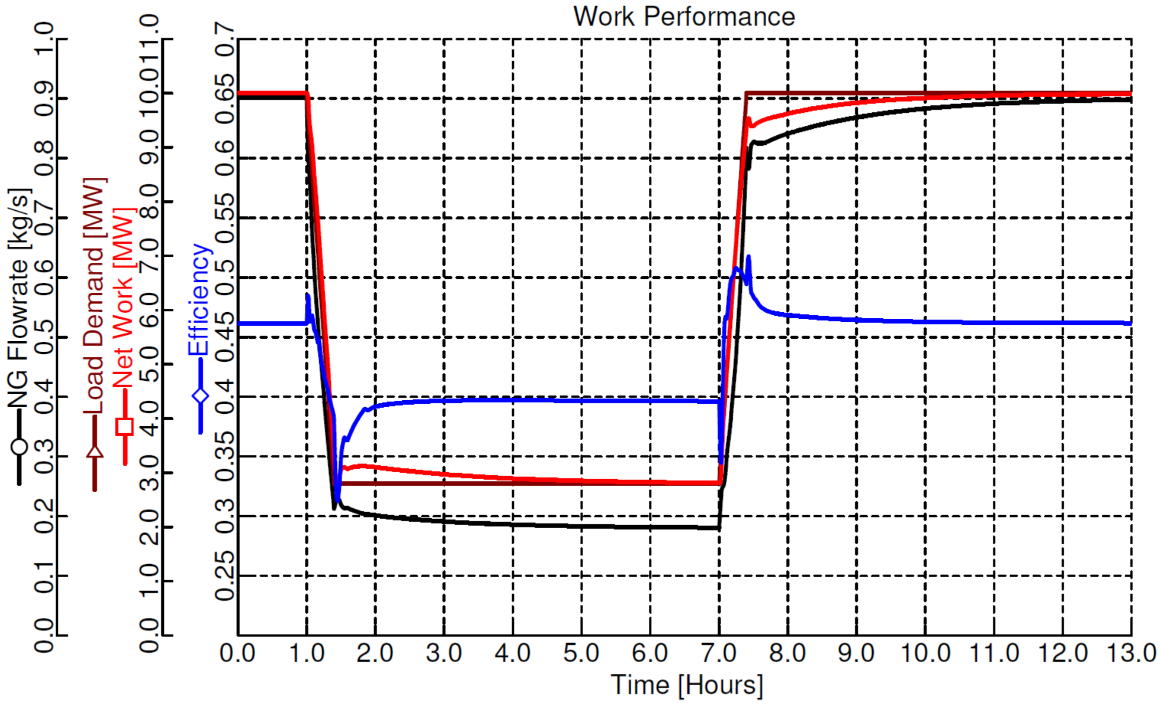

Figure 2. Work performance plot in response to ramp-change (at 3%/min) in MW-demand down to 28% full-load and back to full-load (at similar ramp-rate) with proposed control architecture (with active FSC)

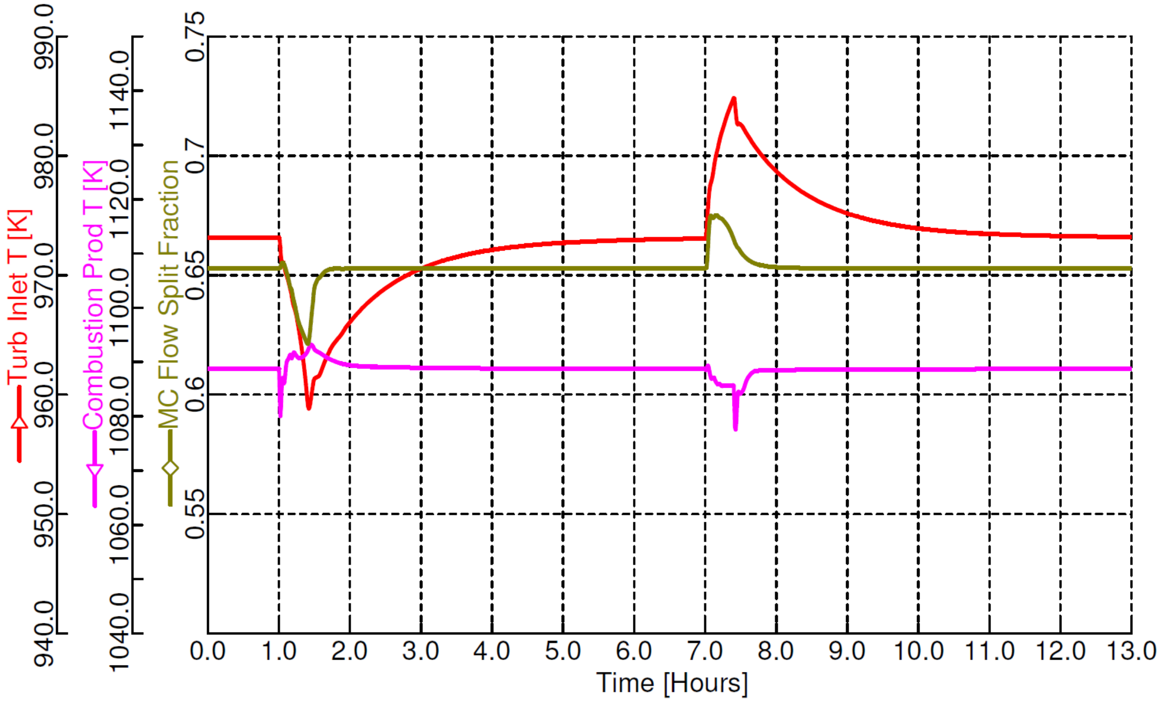

Figure 3. Relevant temperature and MC/BC flow-split plots in response to ramp-change (at 3%/min) in MW-demand down to 28% full-load and back to full-load (at similar ramp-rate) with proposed control architecture (with active FSC)

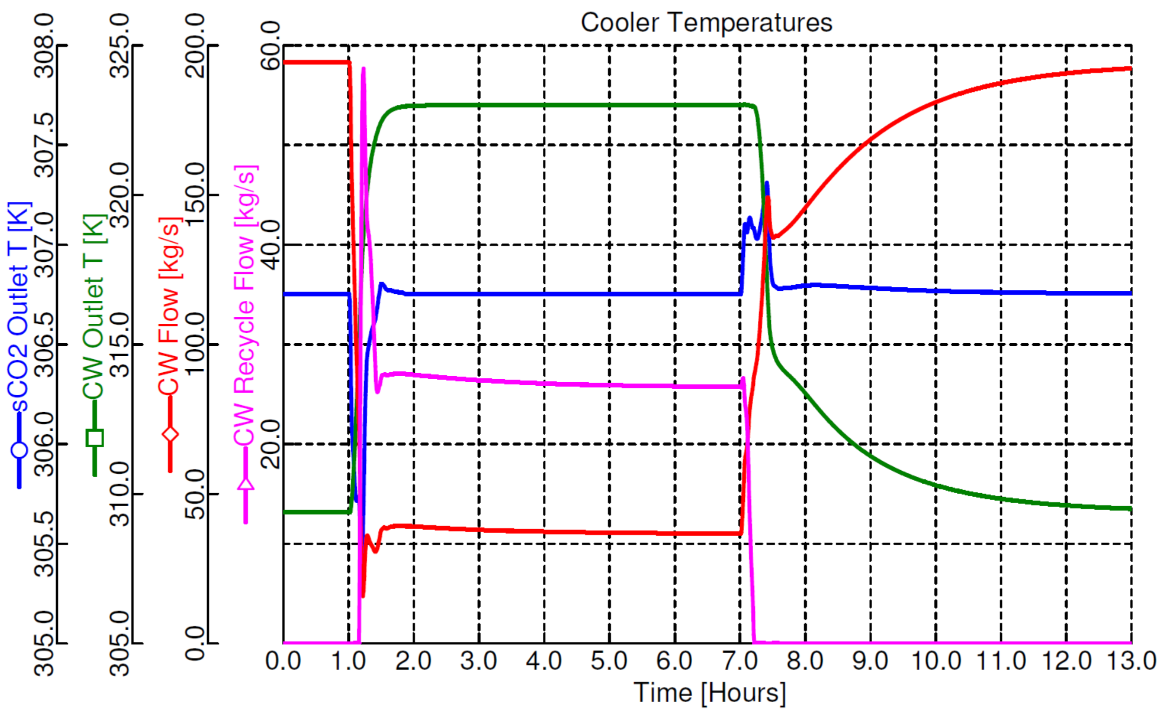

Figure 4. Cooler-related process variable plots in response to ramp-change (at 3%/min) in MW-demand down to 28% full-load and back to full-load (at similar ramp-rate) with proposed control architecture (with active FSC)

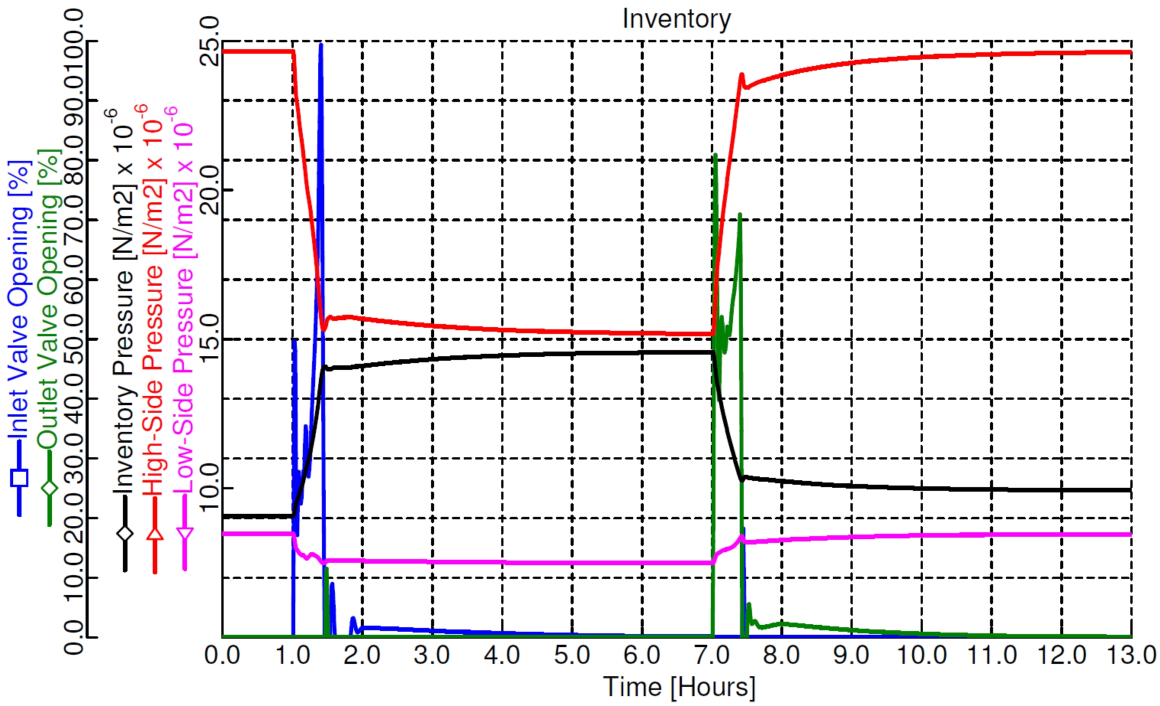

Figure 5. sCO_2 inventory-tank related process variable plots in response to ramp-change (at 3%/min) in MW-demand down to 28% full-load and back to full-load (at similar ramp-rate) with proposed control architecture (with active FSC)

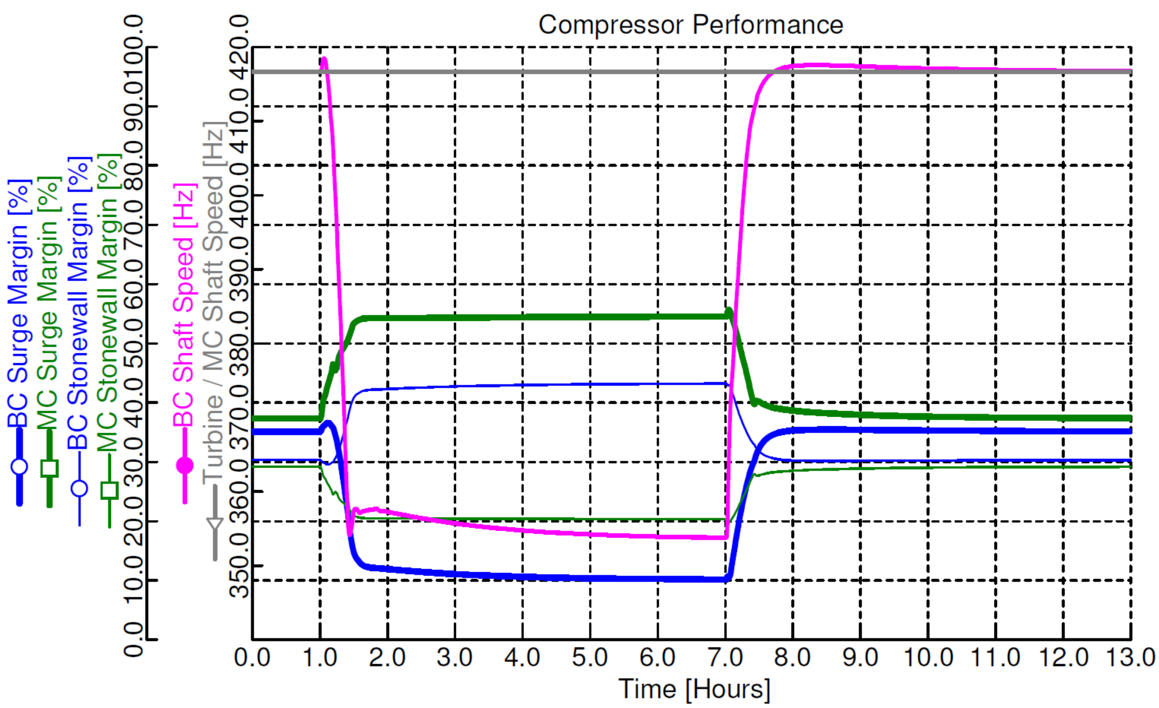

Figure 6. Compressor surge/stonewall margin and turbomachinery shaft-speed plots in response to ramp-change (at 3%/min) in MW-demand down to 28% full-load and back to full-load (at similar ramp-rate) with proposed control architecture (with active FSC)

Control comparison responses with and without flow-split control

This section compares and contrasts the proposed control architecture with and without flow-split control. Figure 7 presents the control responses highlighting the benefits of using FSC, especially through the efficiency subplot, where a 2.5% higher efficiency is observed at 72% turn-down condition. In addition, the efficiency benefits are seen throughout the transient process, even before the part-load steady-state is achieved.

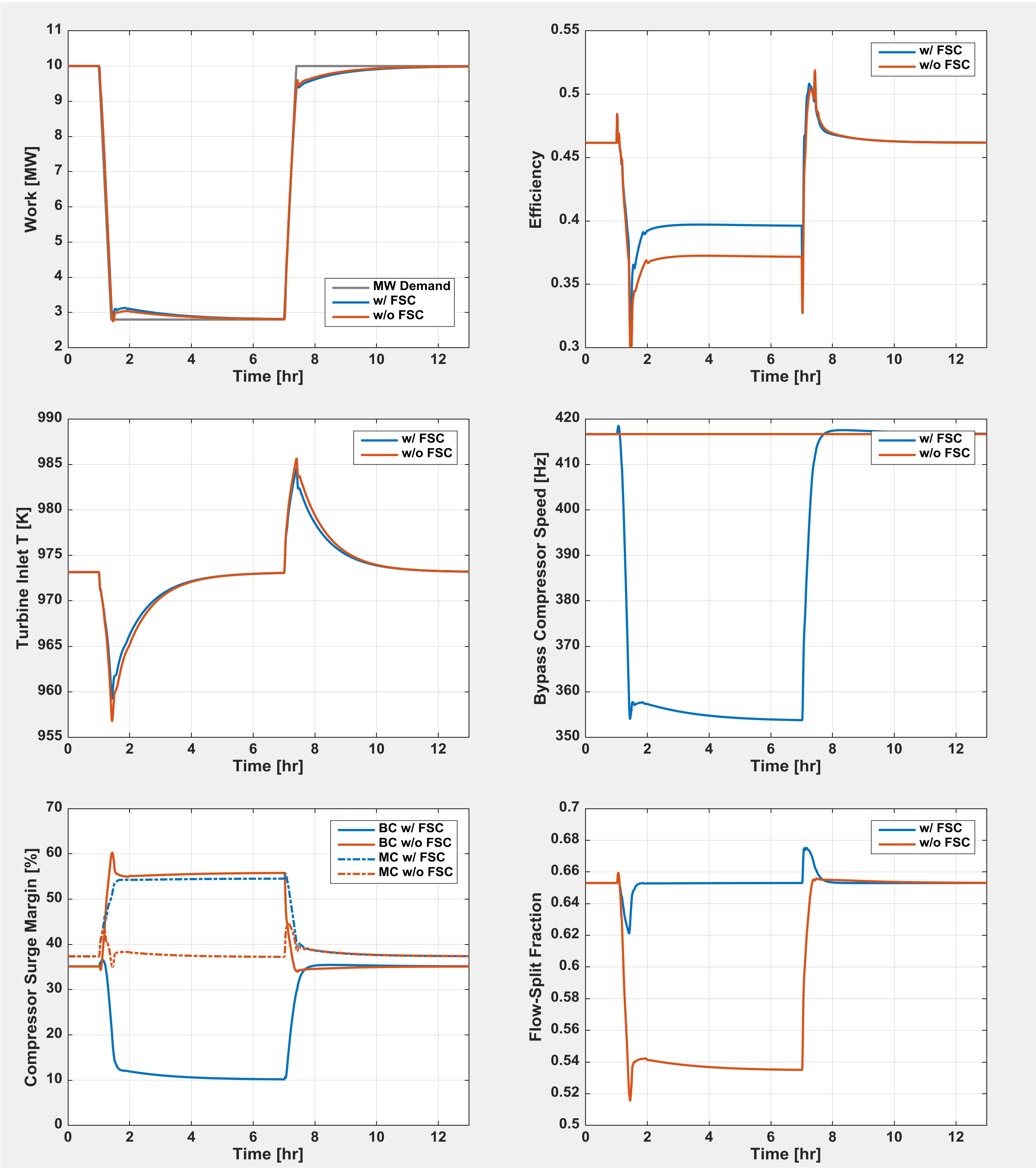

Figure 7. Comparison plots for control responses with and without flow-split control – in response to ramp-change at 3%/min in MW-demand down to 28% full-load and back to full-load at similar ramp-rate

Actual MW and TIT profiles are marginally different. However, the bypass compressor does not approach surge-margin for the non-FSC case as opposed to active FSC. It may be reasonable to state that the transient efficiency benefits of using an FSC far exceed the risks associated with the BC reaching surge especially with an active surge-avoidance logic – very similar to that utilized in this study.

Control responses for large-ramps in fuel flowrate

Control response analysis for large variations in NG fuel-flowrate is necessary to quantify effectiveness of the proposed sCO_2 RCBC control architecture. This section presents dynamic simulation results for 3%/min fuel flowrate ramps in the presence of FSC. Figure 8 shows the fuel ramp-down (introduced at 1 hr) to a very low NG flowrate (81% turn-down) at 3%/min. Similar to the previous studies, the cycle is held at this low-load condition until the process stabilizes. Thereafter, a ramp-up in fuel flowrate is introduced at t = 7 hr with similar ramp rate up to full-load condition. It can be seen that during ramp-down, the efficiency drastically reduces to 34%. Once the fuel-ramp ends, efficiency gradually increases and settles near 39% within a span of 3.5–4 hrs. During ramp-up operation the transients are faster – peaking at 52.5% and settling at design efficiency within 2–3 hrs after ramp-up is introduced. Figure 9 shows a dip in TIT down to 950K with a longer duration for this temperature to reach the design TIT. The slower transients during ramp-up and larger dips in TIT are accounted for by a "pressure-pinch" condition, described later in the text. The TIT peaks at 985K well within the maximum allowable TIT.

Figure 10 show the cooling-water temperature transients. Similar to the previous case, the values during ramp up/down are well controlled and meet constraint objectives. Figure 12 provides plots for surge and stonewall margins through the ramp operations. The transients are similar to previous MW-demand cases. Upon close examination of the BC surge margin and the MC flow-split plots (Figure 9), it can be seen that the BC surge avoidance logic remains active after t = 2 hrs and the flow-split control is sacrificed in favor of the BC surge-margin controlled at 10%. This leads to a marginal dip in flow-split as seen in Figure 9.

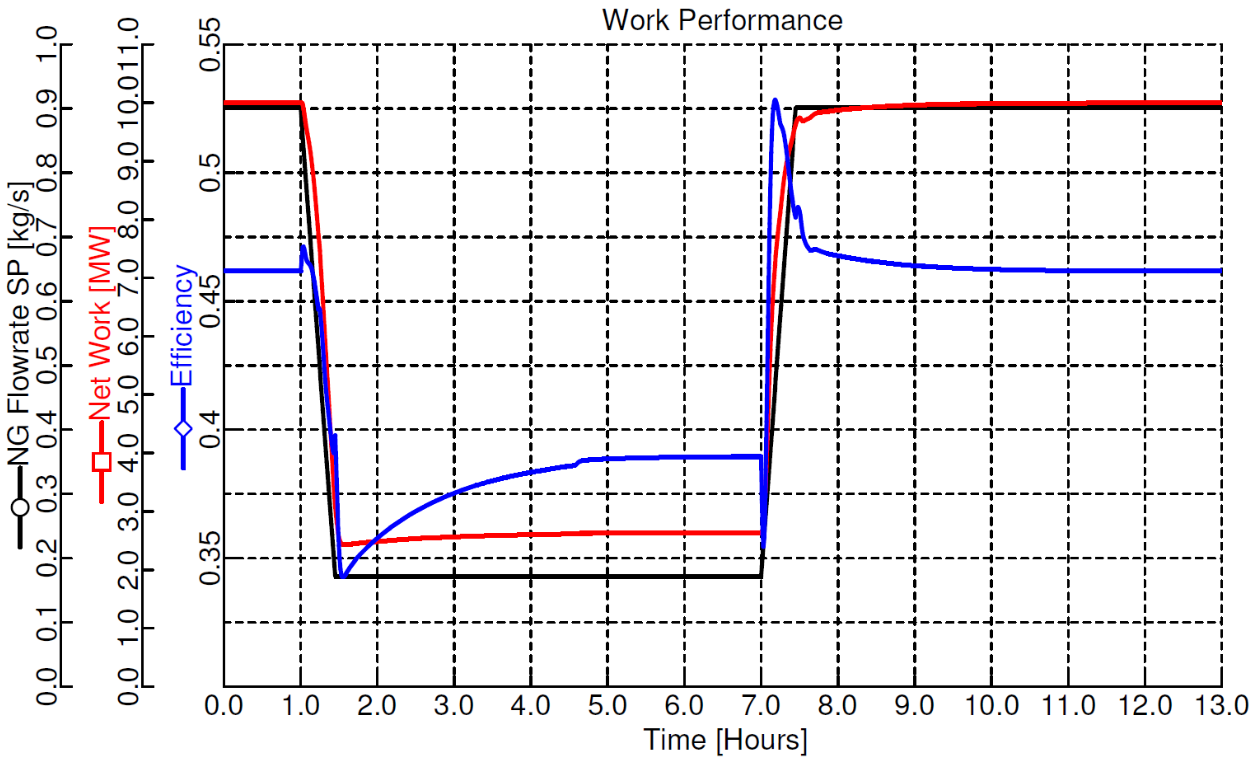

Figure 8. Work performance plot in response to ramp-change (at 3%/min) in fuel-flowrate down to 19% full-load and back to full-load (at similar ramp-rate) with proposed control architecture (with active FSC)

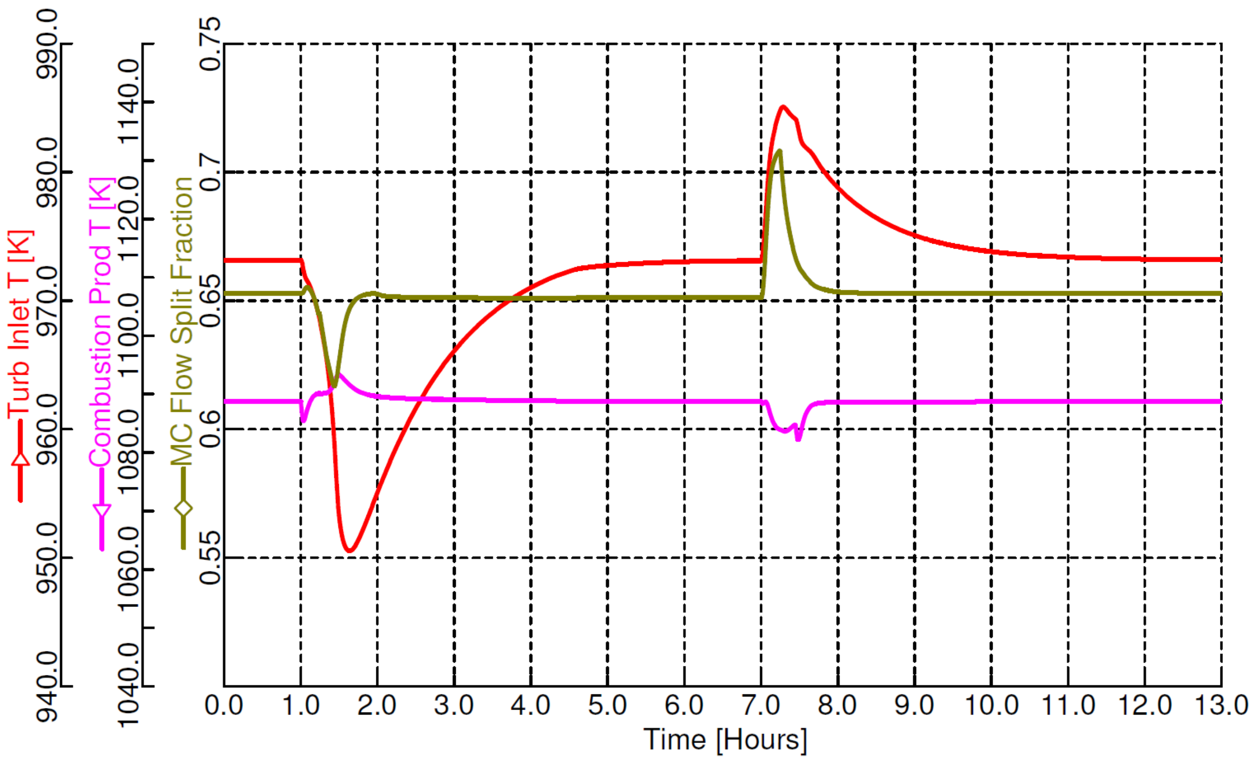

Figure 9. Relevant temperature plots in response to 77%/hr fuel ramp-rate with proposed control architecture (without surge avoidance control)

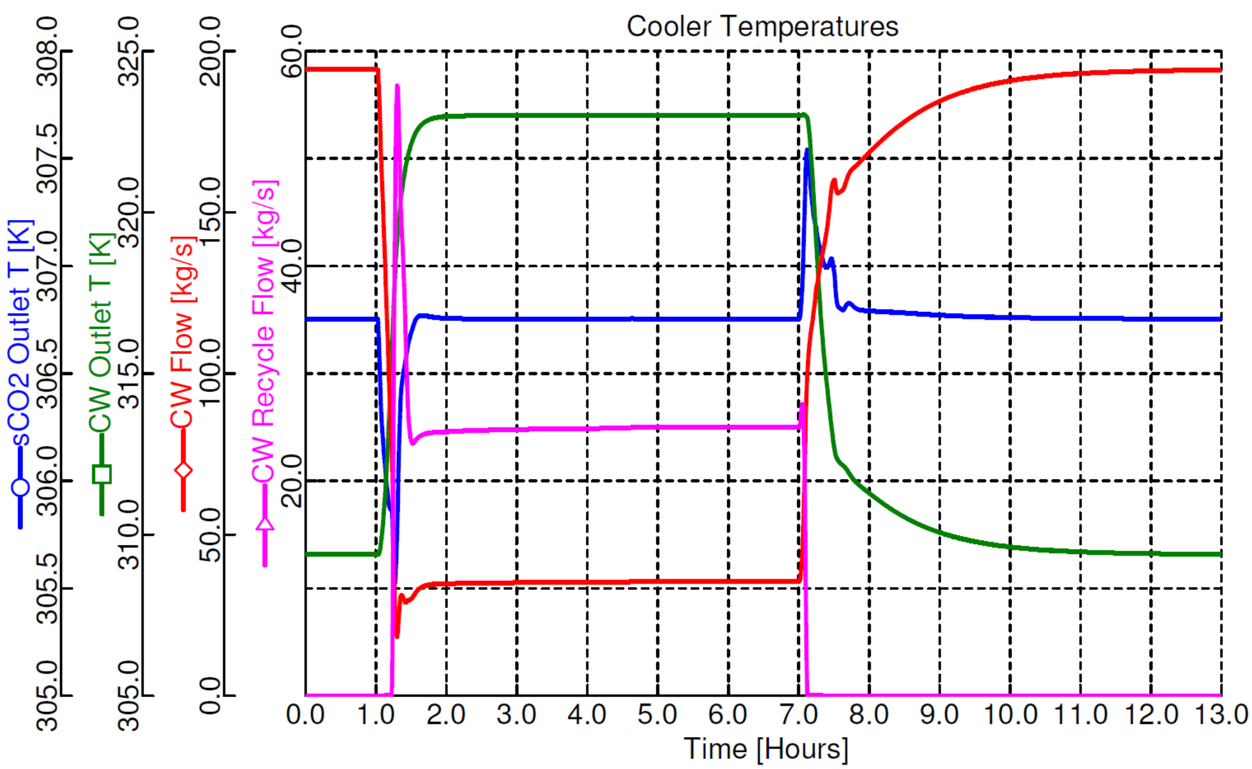

Figure 10. Cooler-related process variable plots in response to 77%/hr fuel ramp-rate with proposed control architecture (without surge avoidance control)

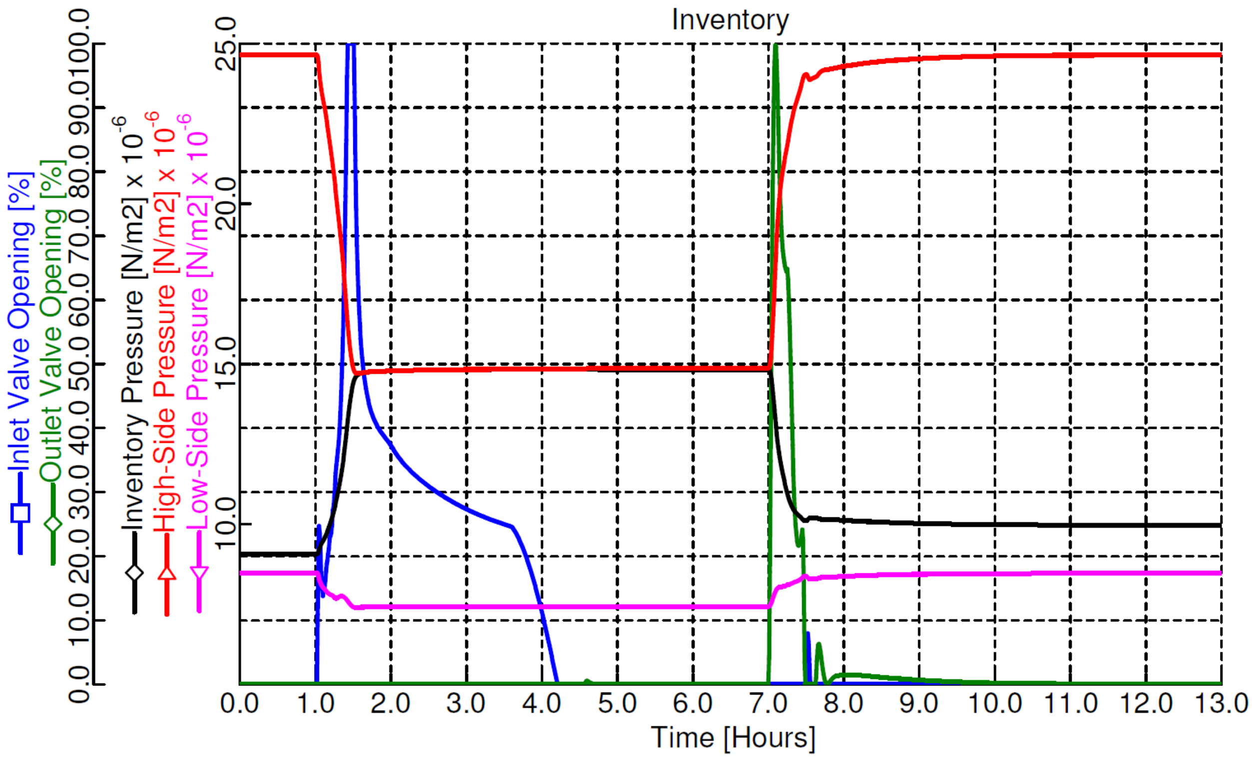

Figure 11. sCO_2 inventory-related process variable plots in response to 77%/hr fuel ramp-rate with proposed control architecture (without surge avoidance control)

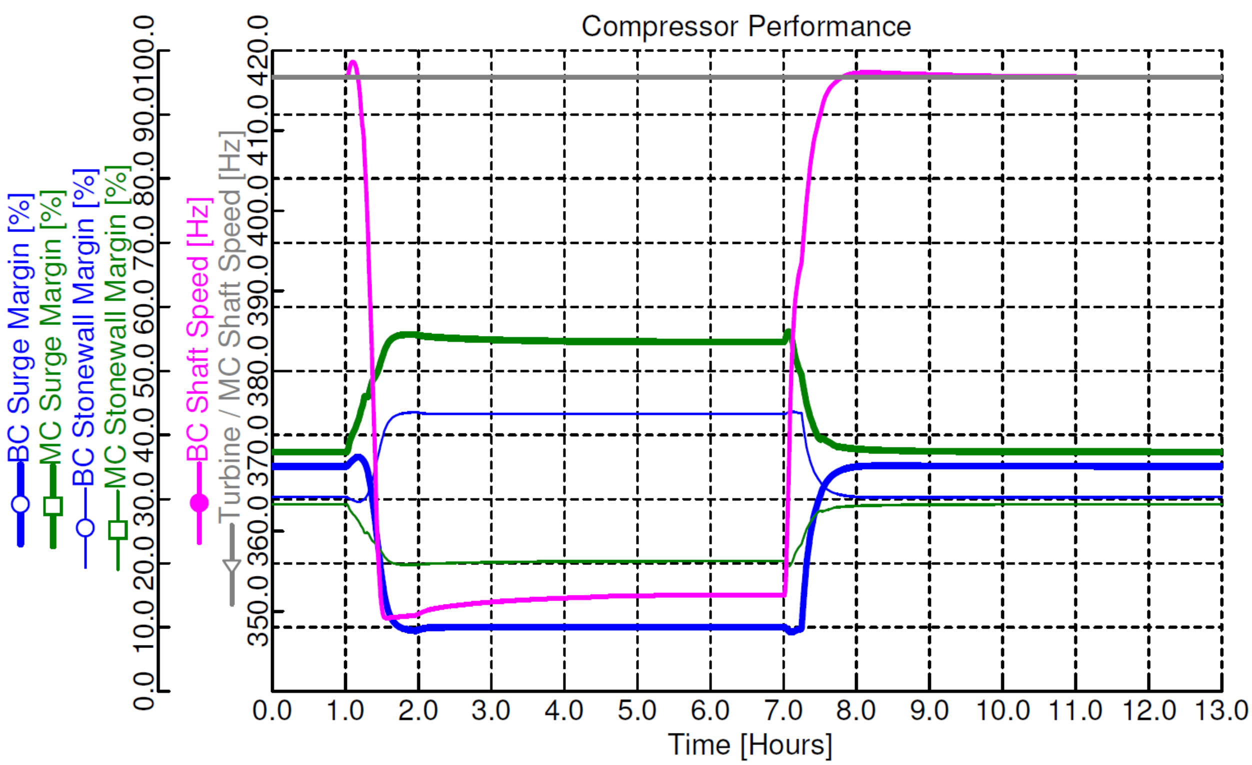

Figure 12. Compressor surge and stonewall margin plots in response to 77%/hr fuel ramp-rate with proposed control architecture (without surge avoidance control)

Pressure pinch between inventory tank and cycle high-side pressure

It must be emphasized that for large turn-downs, the inventory tank pressure reaches saturation with respect to the cycle high-side pressure. Once such a pressure-pinch condition is reached, sCO_2 can no longer be extracted from the cycle. In such an event, the TIT TC keeps increasing the pressure SP to the inventory PC, without any actual sCO_2 removal from the cycle. This in turn renders the TIT non-responsive to the controller action and the TIT may not return to the design temperature. In the previous case study, the 81% fuel-flow turn-down was carefully chosen to demonstrate a "boundary-case" scenario where the system reaches an inventory-tank pressure-pinch condition (see Figure 11) but the TIT is still restored to design temperature (see Figure 9) – leading to a larger dip in TIT as compared to first case study (Figure 3). However, for further turn-down situations, the TIT may not recover and eventually settle at a lower temperature value (below design). This would significantly deteriorate the cycle efficiency. It could be further inferred that once the pressure-pinch is reached at sufficient fuel/MW turn-down, a separate control formulation may be needed to maintain increased cycle efficiency, perhaps by throttling flow through the main-compressor to reduce overall cycle flow, thereby increasing temperatures around the cycle, including the TIT. This strategy is beyond the scope of current work, although it was investigated in the off-design steady-state studies by Zitney and Liese (2018). In an ideal scenario, the tank is sized/designed to accommodate minimum desired continuous load operation (without achieving pressure-pinch) especially when compressor speed control/throttle is not an option. This observation is similar to studies conducted at ANL in Moisseytsev and Sienicki (2011), wherein the authors claim that the range of inventory control is limited by the total inventory tank volume and the speed of inventory control is limited to how fast a distortion of the flow at the compressor outlet and inlet (where inventory control is connected to the cycle) can be applied without having a significant negative effect on compressor operation.

In view of above discussion, it must also be noted that if the TIT TC control-action remains unbounded during a large turn-down, the inventory pressure SP (serving as the manipulated variable, MV for TIT TC) keeps increasing. In the subsequent event of a cycle turn-up, the appropriate corrective action of TC leading to immediate withdrawal of sCO_2 from the tank is significantly delayed owing to a large build-up of previous "integral windup" control action. In the current study, in addition to having an anti-reset-windup within the controller block, an upper constraint of 16 MPa is placed on the TIT TC output. The effect of this is seen in Figure 11, where the inventory inlet valve eventually shuts off without staying wide-open for a prolonged time even though the tank pressure-pinch remains.

CONCLUSIONS

In this work, a regulatory-layer control architecture has been developed and implemented on a pressure-driven dynamic simulation model of a 10MWe sCO_2 recompression Brayton cycle. This study serves as a platform for understanding control-related challenges potentially applicable to the RCBC facility within the STEP program and makes an initial attempt to implement an effective regulatory control through simulation studies. The control objectives were identified and various controllers were formulated to address each of these objectives. It was found that with the controllers in place, the sCO_2 cycle regulated successfully in the face of large 3%/min MW-demand and fuel ramp-rates, while meeting various operating criteria such as maximum allowable turbine-inlet-temperature, maintaining cycle efficiency during transients, preventing high cooling water exit temperatures, maintaining low main-compressor inlet temperatures while operating in the super-critical region, etc. Three case-studies were presented, compared and contrasted – one with a ramp in MW-demand with active flow-split control, the second with a similar ramp study but without flow-split control and the third with a ramp disturbance in fuel flowrate. It was found that the control architecture with flow-split control provided higher cycle efficiency through-out the ramp operation. However, the bypass compressor came close to the allowable surge-margin limit necessitating surge-avoidance logic within the control architecture. Finally, some of the operability/controllability nuances related to inventory-tank pressure-pinch were described and various measures to address them were presented.

FUTURE WORK

Potential future work includes development of control methodologies to further tighten the TIT deviation. This may require some modifications on the combustion temperature by sending in excess air during the transients. An attempt to improve control architecture toward offset-free load tracking during fast ramp-rates will be pursued. In addition, further investigation into techniques to control low-load conditions (close to shut-down) will be pursued. This will involve automating the process of relaxing the TIT below certain load and/or considering the possibility of maintaining TIT for a longer period by ramping down the compressor speed once the inventory tank is filled to its maximum capacity. Furthermore, at such a low load condition where compressor performance is severely degraded, a robust surge-control logic will be developed for both coupled and decoupled turbomachinery. The overall approach will be targeted toward meeting control objectives for attaining faster settling times, higher efficiencies averaged throughout the transients, and lower TIT deviations.

REFERENCES

Aspen Technology, Aspen Custom Modeler®, http://www.aspentech.com/products/aspen-custom-modeler.aspx (2017a).

Aspen Technology, Aspen Plus®, http://www.aspentech.com/products/aspen-plus.aspx (2017b).

Aspen Technology, Aspen Plus Dynamics®, http://www.aspentech.com/products/aspen-dynamics.aspx (2017c).

Carstens, N., "Control strategies for supercritical carbon dioxide power conversion systems." PhD diss., Massachusetts Institute of Technology (2007).

Casella, F. and P. Colonna, "Development of a Modelica dynamic model of solar supercritical CO_2 Brayton cycle power plants for control studies," *Proceedings of the 3rd International Supercritical CO_2 Power Cycles Symposium*, Boulder, CO, May 24-25 (2011).

Conboy, T., J. Pasch, and D. Fleming. "Control of a supercritical CO_2 recompression Brayton cycle demonstration loop," *Journal of Engineering for Gas Turbines and Power*, 135(11), 111701 (2013).

DOE, "Energy Department Announces New Investments in Supercritical Transformational Electric Power (STEP) Program," Department of Energy (DOE), http://www.energy.gov/ne/articles/energy-department-announces-new-investments-supercritical-transformational-electric, December 10 (2015).

Dostal, V., P. Hejzlar, and M.J. Driscoll, "High-Performance Supercritical Carbon Dioxide Cycle for Next-Generation Nuclear Reactors," Nuclear Technology, 154, 265-282 (2006).

Kao, S., J. Gibbs, and P. Hejzlar, "Dynamic Simulation and Control of a Supercritical CO_2 Power Conversion System for Small Light Water Reactor Applications," *Proceedings of the 2nd International Supercritical CO_2 Power Cycles Symposium*, Troy, NY, Apr 29-30 (2009).

Moisseytsev, A. and J.J. Sienicki, "Control System Options and Strategies for Supercritical CO_2 Cycles," Argonne National Laboratory," ANL-GenIV-081 (2006).

Moisseytsev, A. and J.J. Sienicki, "Supercritical Carbon Dioxide Cycle Control Analysis," Argonne National Laboratory," ANL-GenIV-111 (2008).

Moisseytsev, A. and J.J. Sienicki, "ANL Plant Dynamics Code and Control Strategy Development for the Supercritical Carbon Dioxide Brayton Cycle," *Proceedings of the 2nd International Supercritical CO_2 Power Cycles Symposium*, Troy, NY, Apr 29-30 (2009).

Moisseytsev, A. and J. J. Sienicki, “Investigation of Plant Control Strategies for a Supercritical CO_2 Brayton Cycle Coupled to a Sodium-Cooled Fast Reactor using the ANL Plant Dynamics Code,” *Proceedings of the 3rd International Supercritical CO_2 Power Cycles Symposium*, Boulder, CO, May 24-25 (2011).

Pasch, J., T. Conboy, D. Fleming, and G. Rochau, “Supercritical CO2 Recompression Brayton Cycle: Completed Assembly Description,” Sandia Report, SAND2012-9546 (2012).

Singh, R., A.S. Rowlands, and P.A. Jacobs, “Dynamic characteristics and perspectives on control of a supercritical-CO_2 closed Brayton-cycle power-loop in a geothermal power plant,” *Proceedings of the 3rd International Supercritical CO_2 Power Cycles Symposium*, Boulder, CO, May 24-25 (2011).

Trinh, T. Q. "Dynamic response of the supercritical $C0_2$ Brayton recompression cycle to various system transients." PhD diss., Massachusetts Institute of Technology (2009).

White, C., "Analysis of Brayton Cycles Utilizing Supercritical Carbon Dioxide," National Energy Technology Laboratory, DOE/NETL-4001/070114 (2014).

White, C., W. Shelton, and R. Dennis, "An Assessment of Supercritical CO2 Power Cycles Integrated with Generic Heat Sources," Proceedings of the *4th International Supercritical CO_2 Power Cycles Symposium*, Pittsburgh, PA, September 9-10 (2014).

Zitney, S.E. and E.A. Liese, "Dynamic Modeling and Simulation of a 10 MWe Supercritical CO_2 Recompression Closed Brayton Power Cycle for Off-Design, Part-Load, and Control Analysis," Proceedings of the *6th International Supercritical CO_2 Power Cycles Symposium*, Pittsburgh, PA, March 27-29 (2018).

ACKNOWLEDGEMENT AND DISCLAIMER

This technical effort was performed in support of the National Energy Technology Laboratory's ongoing research in Supercritical CO_2 Power Cycle Advanced Sensors Support under the RES contract DE-FE0004000.